

Particle Size Effect on the Filtration Drag of Fly Ash from a Coal Power Plant

Joo-Hong Choi[†], Soon-Jong Ha, Young-Chul Bak and Young-Ok Park*

Department of Chemical Engineering and ERI, Gyeongsang National University, Jinju 660-701, Korea

*Particle Technology Research Center, Korea Institute of Energy Research, Daejeon 305-343, Korea

(Received 22 April 2002 • accepted 2 September 2002)

Abstract—In order to investigate the filtration properties of fly ash from a conventional coal power plant, the filtration drag across the dust cake over an absolute fiber-glass filter element was measured. A fluidized bed column was utilized to obtain a well characterized particle stream. The cake resistance coefficient was analyzed by the equation proposed by Endo et al. [1998] in order to observe the effect of particle size and polydispersity. The filtration drag was measured for three kinds of particle stream having the geometric mean particle size of 3.15, 6.07, and 7.83 μm and the geometric standard deviation less than 1.44 in the practical operation conditions for the field applications of face velocity of 0.03-0.06 m/s and area dust load up to 0.2 kg/m^2 . A dust cake of smaller particle size showed larger pressure drop even though the porosity was higher and presented high compressibility according to the face velocity. The particle polydispersity was also a dominant factor affecting the compressibility of the dust cake.

Key words: Gas Filtration, Particle Size Effect, Fly Ash, Compressibility, Polydisperse Particle

INTRODUCTION

Most conventional coal power plants have utilized an electric precipitator to control particles. However, recently, filtration using bag filters has been demonstrated as a more useful technology for meeting the strict regulation limits for fine particle emission with high collection efficiency and without the side effect to form toxic gases like dioxins [Choi et al., 2002]. So it is very interesting in characterization of the filtration properties of fly ash from a coal power plant.

The pressure drop is a key factor for the design and operation of the filter system. In normal operation, the filter element should be cleaned periodically when the pressure drop of the system reaches a tolerable limit. The pressure drop originates from the drag forces across the filter media and the dust cake. Fine particles tend to penetrate into the pores of the filter media on the conditioning step and plug the filter media or slip out in the clean gas stream. The filter element conditioned has a permanent dust layer that has a role for additional filtration function. The resistance coefficient of the permanent layer is usually more than 10 times the value of the fresh bag filter element. However, it is usually negligible relatively to that across the transition dust layer when the thickness is greater than about 2 mm [Perry and Green, 1973]. Pressure drop across the dust cake dominantly depends on its structure represented by the cake porosity. However, in spite of many studies on the gas/solid filtration, the accurate prediction of the filtration performance for a special system is not easy because it is multi-dependent on many factors from particle (shape, size, and density), gas (viscosity and humidity), and the filtration conditions (face velocity and cleaning methods) [Aguar and Coury, 1996; Cheung and Tsai, 1998; Choi et al., 2002]. Theoretically, several equations [Aguar and Coury, 1996; Endo et al., 1998; Gupta et al., 1996; Neiva et al., 1999] predict the pressure drop increase as the particle size is smaller. Particle poly-

dispersity and shape factor are also dominant factors of the filtration drag [Endo et al., 1998; Gupta et al., 1996; Perry and Green, 1973]. The equations proposed indicate that the dust cake of high porosity leads the low value of pressure drop. However, the pore size is an important factor affecting the filtration drag if we consider the fact that small particles form a dust cake of high porosity but reveals a higher pressure drop than that of large ones.

Theoretically, filtration drag is expressed linearly with the area dust load at constant face velocity. However, several papers [Aguar and Coury, 1996; Höflinger et al., 1994; Schmidt, 1995, 1997] reported the curvature dependences of it, which show the compression effect with the increase of the dust cake. Face velocity is also a dominant factor on the compression effect of dust cake [Silva et al., 1999]. Cheung and Tsai [1998] correlated the specific cake resistance coefficient (k_2) and the face velocity with the equation $k_2 = fV_f^n$, where f and n are constants. They reported that several fly ashes showed a wide range of the n value from about 0.5 to 0.75. These variant results seem to be due to the different properties of the particles on the factors of particle size, composition and shape factor or the measuring conditions because many factors are co-related. So the uncertainty on the characterization of particles as well as the experimental conditions need to be eliminated in order to get a reliable data. Actually, it is difficult to prepare a uniform feed stream of fine particles because they tend to be aggregated or be badly distributed in the small experimental unit.

In this study we prepared a well characterized and distributed dust stream using a fluidized bed column. The gas stream, which contained a special range of particle sizes, was directly introduced into the test column in order to investigate the effects of particle size on the filtration.

THEORY OF PRESSURE DROP DURING THE FILTRATION

The total pressure drop (ΔP_t) of the filtration that is expressed

[†]To whom correspondence should be addressed.

E-mail: jhchoi@nongae.gsnu.ac.kr

by Eq. (1) denotes the sum of those across the filter element (ΔP_f) and the dust cake (ΔP_c). Where, k_1 and k_2 are the resistance coefficients across the conditioned filter element and the dust layer, respectively, in the normal operation. The filter drag (S) represents the value of the pressure drop across the dust cake over the face velocity (V_f) like Eq. (2). It depends almost linearly on the value of the area dust load (W) for the conditioned filter [Cheung and Tsai, 1998; Neiva et al., 1999]. The filter drag coefficient (k_2) of the equation is the key factor to monitor the property of the dust cake. And it has a correlation with factors of porosity (ϵ), gas viscosity (μ), particle density (ρ), dynamic shape factor (κ), geometric mean diameter (d_g), and geometric standard deviation (σ_g) as Eq. (3) for the polydisperse particle [Endo et al., 1998].

$$\Delta P_f = \Delta P_f + \Delta P_c = k_1 V_f + k_2 V_f W \quad (1)$$

$$S = \frac{\Delta P_c}{V_f} = k_2 W \quad (2)$$

$$k_2 = \frac{18\mu\kappa v(\epsilon)}{\epsilon^2} \cdot [\rho_p d_g^2 \exp(4\ln^2 \sigma_g)]^{-1} \quad (3)$$

$$k_2 = \frac{180\mu\kappa(1-\epsilon)}{\epsilon^3} \cdot [\rho_p d_g^2 \exp(4\ln^2 \sigma_g)]^{-1} \quad (4)$$

$$k_2 = \frac{180(1-\epsilon)}{\epsilon^3} \cdot [\rho_p \phi_s^2 d_s^2]^{-1} \cdot \mu \quad (5)$$

The void function, $v(\epsilon)$ depends on porosity of the dust cake and is obtained by experiment. If $v(\epsilon)$ is $10(1-\epsilon)/\epsilon$, Eq. (3) is expressed as Eq. (4) and is similar form with the Kozeny-Carman equation like Eq. (5) for monodisperse particle which is expressed by Neiva et al. [1999]. Where ϕ_s is particle shape factor. So Eq. (4) is very reasonable and useful to represent the effect of particle shape and polydispersity. Endo et al. [1998] reported Eq. (3) showed the best

fit for four types of powder: Arizona road dust ($d_p=2\mu\text{m}$ and $\kappa=1.5$), alumina particle ($d_p=2\mu\text{m}$ and $\kappa=1.05$), alumina particle ($d_p=0.7\mu\text{m}$ and $\kappa=1.05$), and talc particle ($d_p=2.3\mu\text{m}$ and $\kappa=2.04$).

EXPERIMENTAL

Fig. 1 shows the schematic diagram of the experimental unit. The fly ash was classified in the fluidized bed column using dry air at room temperature. About 0.001 m^3 of fly ash was filled initially and blew out at the superficial velocity of 0.04, 0.13, and 0.17 m/s. So particles having a settling velocity smaller than the superficial velocity are blown out from the bed. A part of this outlet stream was first chosen as the particle stream for fine particles. The fine particles under the superficial velocity were eliminated by being blown out for about two hours after the first experiment. The second and third classes of particles were prepared sequentially with the same method. The fly ash used in the experiment is originated from a conventional coal power plant and contains unburned carbon of about 5%. Its chemical composition of SiO_2 , Al_2O_3 , Fe_2O_3 , CaO , SO_3 , and TiO_2 were 49.0, 29.4, 6.0, 5.4, 0.9, and 1.6%, respectively. Most of the classified-particles were spherical according to the SEM images with the shape factor of 0.91 [Choi et al., 2002]. Part of dust stream was introduced into an aerodynamic particle size analyzer (API Aerosizer) from the top of the test column in order to measure directly the particle size distribution. A glass fiber filter element (Gelman Sci., A/B 66209) of the disk type (0.047 m diameter) was mounted in the filter holder placed in the counter current direction toward the dust stream. Its effective filter area is 0.001256 m^2 . The aerosol retention (by ASTM D 2986-71) of the filter element is 99.9999% according to the data by the maker. A fresh filter element was utilized for each run. And the pressure drop across the dust cake formed on the filter element was recorded with time variance after the dust stream was introduced into the test column in order to obtain the curve for the pressure drop versus time (ΔP -t curve) at a constant face velocity. The face velocity across the filter element was controlled with a mass flow controller connected to the vacuum pump. So the face velocity is constant during the pressure drop measurement even though the pressure drop increases with the time. The total mass of the dust load during the filtration

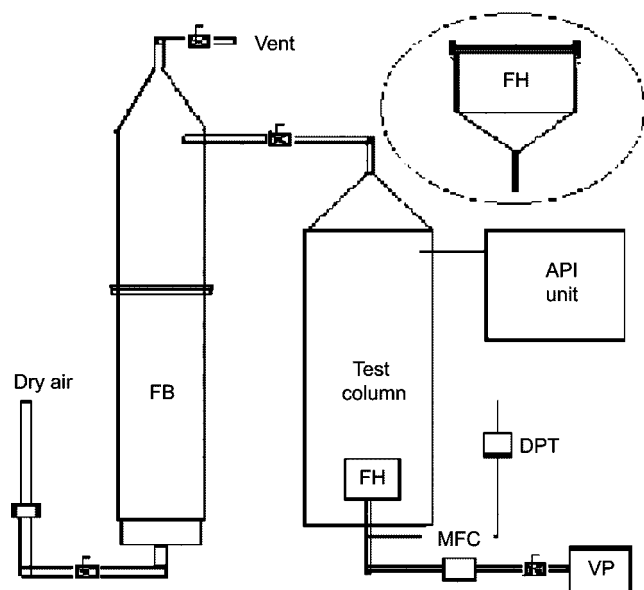


Fig. 1. The experimental unit for the filtration test.

F/B: Fluidized bed
F/H: Filter holder
MFC: Mass flow controller
FM: Flow meter
DPT: Differential pressure transmitter
VP: Vacuum pump

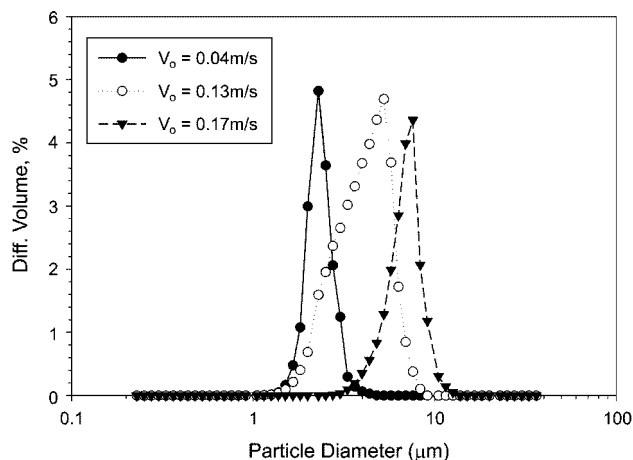


Fig. 2. Particle size distribution of dust sample classified at various V_o .

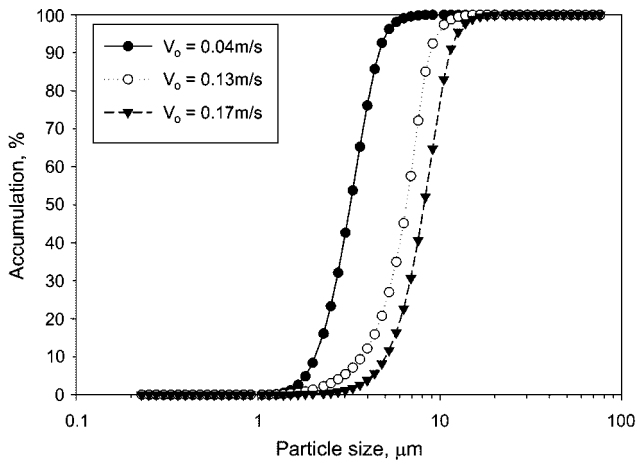


Fig. 3. Accumulative size distribution of particle classified at various V_o .

was weighed to calculate the area dust load on the filter element. The dust was loaded linearly with time during the run of about 30 minutes. The experimental data of ΔP -t curve was converted to the curve of filter drag vs. area dust load (S-W curve).

RESULTS AND DISCUSSION

Fig. 2 and Fig. 3 show the particles are clearly classified at the given superficial velocity with narrow distribution. The physical properties of the fly ashes; geometric mean diameter (d_g), Sauter diameter (d_s), volume average mean diameter (d_v), maximum particle size (d_{gm}), and geometric standard deviation (σ_g) were directly measured by API aerosizer and shown in Table 1. Particle density (ρ_p) was measured with a Le Chatelier’s density bottle. The dynamic shape factor (κ) was calculated by the equation of $(d_v/d_g)^2$ [Hinds, 1999]. And the largest geometric particle sizes (d_{gc}) were calculated by the Eq. (6) based on Stokes’ law. Where μ is air viscosity (1.8×10^{-5} kg/m-sec), V is terminal velocity (m/s), ρ is density of water ($1,000$ kg/m³), and g is gravitational acceleration (9.8 m/s²). The largest geometric particle sizes (d_{gc}) at a terminal velocity corresponding to V_o are larger than the largest one measured (d_{gm}). It is very reasonable that the actual particle blown out is smaller than the one calculated because the superficial velocity is higher than that of terminal velocity.

$$d_{gc} = \sqrt{\frac{18\mu V}{\rho g}} \tag{6}$$

When starting with fresh filter element, the conditioning pattern depends on the filter element as shown in Fig. 4 that represents the typical S-W curves for the particle of $d_g=7.83$ at a face velocity of 0.06 m/s. The metal filter element here is fabricated with metal fiber meshes and composed with three layers. It forms a depth filter ele-

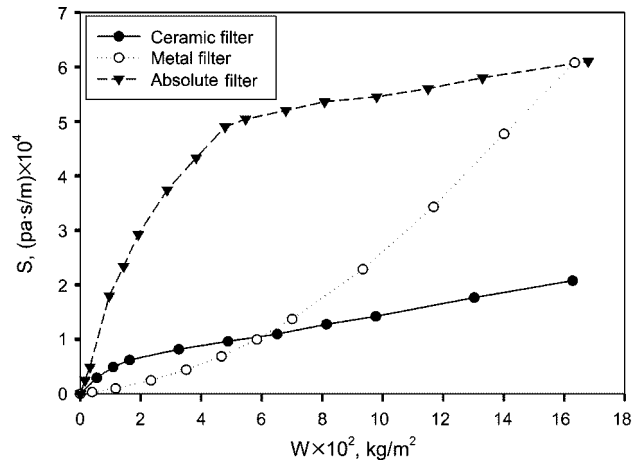


Fig. 4. Patterns of filtration drag according to the filter element.

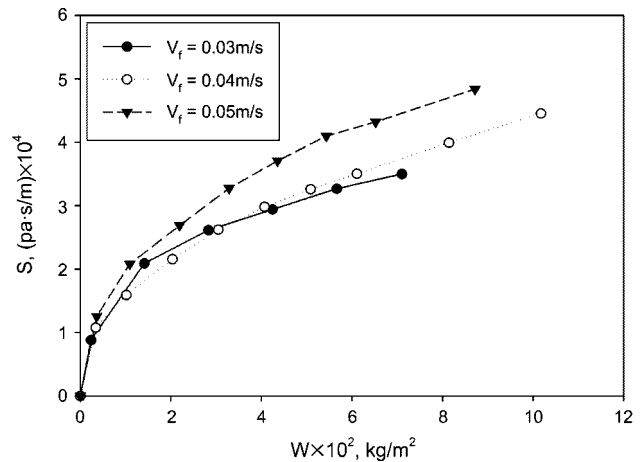


Fig. 5. S-W curves showing the effect of face velocity (for $d_g=3.15$ μm).

ment with average pore size of about 100 μm . The ceramic filter is a DIA-Schumalith 10-20 fabricated by Schumacher Co. It is an asymmetric ceramic filter of SiC material with a thin outer ceramic membrane (100 - 200 μm) of which mean pore size is about 10 μm [Schulz and Durst, 1994]. S-W curve for metal filter element of depth type showed the upward curvature at initial time of dust load and tended to approach the linear curve at high load after the filter element was conditioned. The conditioning time is long because the pores of the depth metal filter element are gradually plugged with the penetrating particles. The high tendency of the upward curvature implies high compression of the dust layer or high plugging of the filter element by the dust particles. In case of absolute fiber-glass filter and rigid ceramic filter elements, the S-W curve presents downward curvature at the initial conditioning step and is con-

Table 1. Physical properties of PC ash classified

V_o [m/s]	ρ_p [kg/m ³]	d_g [μm]	d_s [μm]	d_v [μm]	d_{gm} [μm]	d_{gc} [μm]	σ_g [μm]	κ [-]
0.04	3,020	3.15	3.00	3.31	8.7	23.5	1.37	1.26
0.13	2,500	6.07	5.62	6.44	15.8	47.5	1.44	1.31
0.17	2,380	7.83	7.36	8.25	22.0	48.4	1.40	1.26

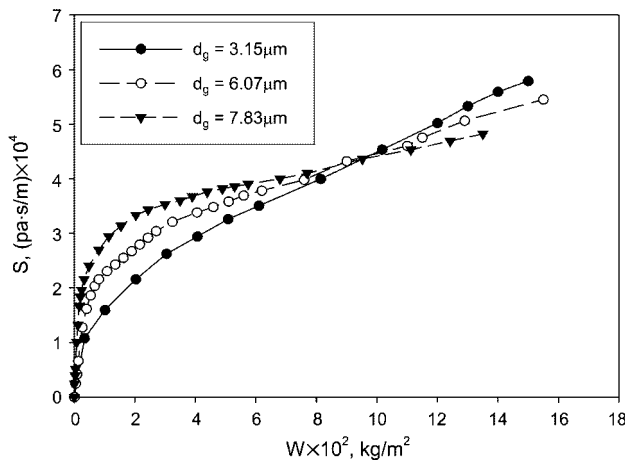


Fig. 6. S-W curves showing the effect of particle size at $V_f=0.04$ m/s.

ditioned quickly. So the absolute fiberglass filter was utilized in the study.

Fig. 5 and Fig. 6 show the typical S-W curves for the fly ash over the absolute filter element. Filter drag of larger particle increases more rapidly than that of smaller one in the conditioning step. However, the increasing rate of S-W curve after the conditioning step is smaller for the larger particle representing a low value of k_2 for the large particle size. The reason for this result is that particles of larger size cover the filter surface more quickly at the initial stage and cause the rapid pressure drop. S-W curves showed almost a linear plot after the area mass load of about 0.07 kg/m^2 . Table 2 presents the k_2 values calculated by Eq. (2) in the linear region of S-W curve for the different particle size and face velocity. If k_2 is expressed by the equation $k_2=fV_f^n$, the constant n implies the compressibility of the dust cake according to the face velocity. Fig. 7 shows the best fitting of the relation. The constant n values were 0.493, 0.477, and 0.405 for the particles size (d_g) of 3.15, 6.07, and $7.83 \mu\text{m}$, respectively. They are slightly lower than the value of 0.5 and 0.517 reported by Dennis and Dirgo [1981] and Cheung and Tsai [1988] for coal fly ash [Cheung and Tsai, 1998], respectively. One possible reason for the different result is due to the different particle size distribution (polydispersity). Cheung and Tsai [1988] used the fly ash of mass median aerodynamic diameter of $5.72\text{--}6.71 \mu\text{m}$ and high geometric standard deviation of $1.91\text{--}2.11$ containing the largest particle size about $100 \mu\text{m}$. The particles used in this study were well characterized with the geometric standard deviation of $1.37\text{--}1.44$ and with the maximum particle size (d_{gm}) of less than $48.4 \mu\text{m}$. According to Eq. (4), the geometric standard deviation lowers the k_2 value, which means that the pressure drop across the dust cake decreases with increase of σ_g . Otherwise, σ_g has also a rela-

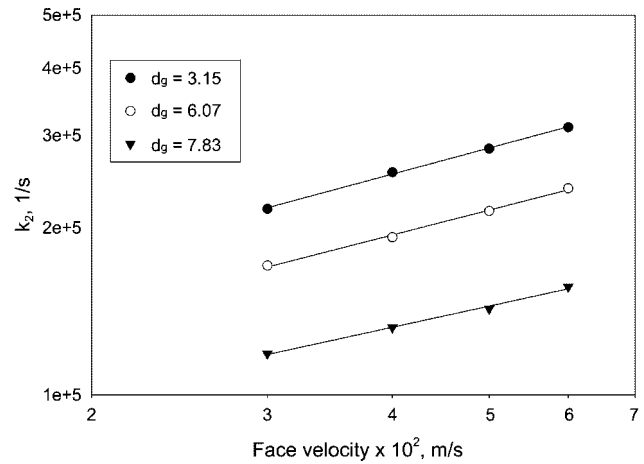


Fig. 7. The correlation curves of k_2 with the face velocity.

tionship with the dust cake compressibility denoted by the n value. The discussion above indicates that dust cake of larger σ_g is more compressible according to the face velocity than that of smaller one.

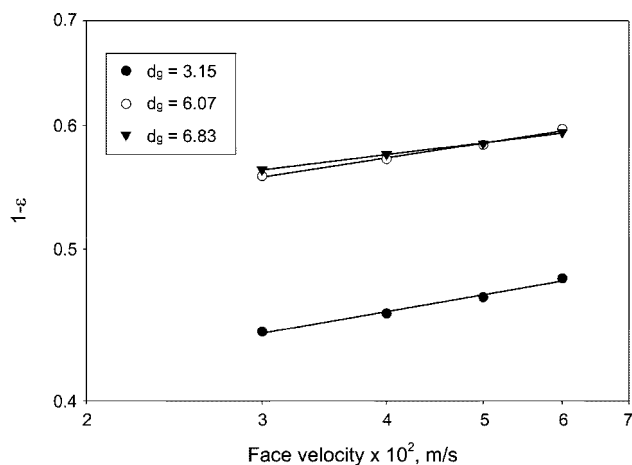
In order to observe the particle size effect on the compressibility of the dust cake, the average porosity (ϵ) of the dust cake was calculated by Eq. (4) and listed in Table 3. It increases with the decrease in the particle size even though the filtration drag is higher than that of larger one. This result means that the filtration drag is more closely affected by the pore size than the porosity of the dust cake. The cake porosity decreases with increasing of the face velocity because the pore is compacted with the increase of the drag force at high face velocity. The relation between the porosity and the face velocity was well correlated by the equation, $1-\epsilon=aV_f^b$, as shown at Fig. 8, where constant b is a kind of compressibility factor of the dust cake influencing with the face velocity. The experimental results show b becomes smaller as the particle size increases, which means that a dust cake of small particles is more compressible than that of larger ones. The b value obtained in this study is in the range of about 0.1, which is lower than the value of about 0.45 reported by Cheung and Tsai [1998]. The experimental result shows that the change of dust cake porosity measured in this study is less sensitive to the face velocity. The different result arises from the reason the dust thickness operated in this study is lower less than 3 times of that observed by Cheung and Tsai [1998]. The maximum area dust load (W) is about 0.2 kg/m^2 in this study. It is a very practical range for the actual field operation of a bag house. And the experimental condition of Cheung and Tsai [1998] was externally extended toward the high dust load and was affected too much with the cake thickness. The dust cake becomes compacted gradually with the increasing of the dust load [Aguar et al., 1996; Neiva et al., 1999]. So the value of

Table 2. The effect of the face velocity on $k_2 (\times 10^{-5})$ and constant f and n for $k_2=fV_f^n$

d_g [μm]	k_2 [1/s]				f [$\text{s}^{n-1}/\text{m}^n$]	n [-]
	$V_f=0.03$ m/s	$V_f=0.04$ m/s	$V_f=0.05$ m/s	$V_f=0.06$ m/s		
3.15	2.31	2.57	2.84	3.09	1,287,000	0.493
6.07	1.74	1.95	2.18	2.48	1,015,000	0.477
7.83	1.19	1.33	1.44	1.58	759,100	0.405

Table 3. The effect of the face velocity on the porosity (ϵ) and constant a and b for $1-\epsilon=aV_f^b$

d_g [μm]	ϵ [-]				a [m/s] ^b	b [-]
	$V_f=0.03$ m/s	$V_f=0.04$ m/s	$V_f=0.05$ m/s	$V_f=0.06$ m/s		
3.15	0.557	0.545	0.534	0.521	0.391	0.115
6.07	0.443	0.429	0.417	0.403	0.499	0.100
7.83	0.438	0.425	0.416	0.406	0.515	0.079

**Fig. 8. The correlation curves of $f(1-\epsilon)$ with the face velocity.**

porosity discussed in the study is an average one through the total thickness of the dust cake. Therefore, there remains the task to measure the porosity directly in the experimental conditions to obtain reasonable data for compression effects. From the views of the overall trend, small particles are more compressible by the effect of face velocity than larger ones.

CONCLUSIONS

The filtration drag of fly ash from a conventional coal power plant was measured to investigate the effects of particle size over an absolute fiberglass filter element. The fly ash of different particle size was prepared in a fluidized bed column and showed the well characterized particle stream for the dust feed of the experimental unit. The cake resistance coefficient, k_2 for the different particle size and face velocity was observed. The average cake porosity was analyzed by the equation proposed by Endo et al. [1998] in order to observe the effect of particle polydispersity.

The cake resistance coefficient, k_2 was increased with decreasing the particle size and increased in the face velocity. And the average porosity of dust cake was increased with decreases in the particle size and with increases in the face velocity. The compressibility constant n expressed by the equation, $k_2=fV_f^n$, decreased with increases in particle size and had a value of 0.4-0.5, which is slightly lower than that reported by others. This discrepancy in the n value implies that the geometric standard deviation representing the polydispersity of the particle distribution was also one of the dominant factors affecting the compressibility of the dust cake. The trend of the compression presented by the cake porosity showed that the porosity of the dust cake decreases almost exponentially according

to the face velocity for a dust cake of small thickness.

ACKNOWLEDGEMENTS

The authors would like to thank the Korea Energy Management Corporation, Korea Institute for Energy Research, and Institute for Advanced Engineering for their financial support.

NOMENCLATURE

- a, b, f, n : constants
 d_g : geometric mean particle size [μm]
 d_{gc} : geometric mean particle size calculated [μm]
 d_{gm} : geometric mean particle size measured [μm]
 d_s : sauter mean particle size [μm]
 d_v : volume average mean particle size [μm]
 k_2 : filter drag coefficient [s^{-1}]
 S : filter drag [$\text{Pa}\cdot\text{s}\cdot\text{m}^{-1}$]
 V : terminal velocity [$\text{m}\cdot\text{s}^{-1}$]
 V_f : face velocity [$\text{m}\cdot\text{s}^{-1}$]
 V_o : superficial velocity in fluidized bed [$\text{m}\cdot\text{s}^{-1}$]
 W : area dust load on the filter element [$\text{kg}\cdot\text{m}^{-2}$]
 ΔP_C : pressure drop across the dust layer [Pa]
 ΔP_F : pressure drop across the filter layer [Pa]
 ΔP_T : total pressure drop [Pa]
 ϵ : porosity [-]
 κ : dynamic shape factor [-]
 μ : air viscosity [$\text{kg}\cdot\text{s}^{-1}\cdot\text{m}^{-1}$]
 ρ_p : particle density [$\text{kg}\cdot\text{m}^{-3}$]
 ρ : water density [$\text{kg}\cdot\text{m}^{-3}$]
 σ_g : geometric standard deviation [μm]
 ϕ_s : shape factor of particle [-]

REFERENCES

- Aguar, M. L. and Coury, J. R., "Cake Formation in Fabric Filtration of Gases," *Ind. Eng. Chem. Res.*, **35**, 3673 (1996).
 Cheung, Y. H. and Tsai, C. J., "Factors Affecting Pressure Drop Through a Dust Cake During Filtration," *Aerosol Science and Technology*, **29**, 315 (1998).
 Choi, J. H., Ha, S. J. and Park, Y. O., "The Effect of Particle Shape on the Pressure Drop across the Dust Cake," *Korean J. Chem. Eng.*, in pressed (2002).
 Choi, H. K., Park, S. J., Lim, J. H., Kim, S. D., Park, H. S. and Park, Y. O., "A Study on the Characteristics of Improvement in Filtration Performance by Dust Precharging," *Korean J. Chem. Eng.*, **19**, 342 (2002).
 Dennis, R. and Dirgo, J. A., "Comparison of Laboratory and Field De-

- rived K₂ Values for Dust Collected on Fabric Filters," *Filtration and Separation*, **18**, 394 (1981).
- Endo, Y., Chen, D.-R. and Pui, D. Y. H., "Effect of Particle Polydispersity and Shape Factor During Dust Cake Loading and Air Filters," *Powder Technology*, **98**, 241 (1998).
- Gupta, A., Novick, V. J., Bisawas, P. and Monson, P. R., "Effect of Humidity and Particle Hygroscopicity on the Mass Loading Capacity of High Efficiency Particulate Air (HEPA) Filters," *Aerosol Science and Technology*, **19**, 94 (1993).
- Hinds, W. C., "Aerosol Technology 2nd ed.," Powells Books, (1999).
- Höflinger, W., Stöcklmyer, Ch. and Hackl, A., "Model Calculation of the Compression Behaviour of Dust Filter Cakes," *Filtration & Separation*, **December**, 807 (1994).
- Neiva, A. C. B., Goldstein, Jr. L. and Calvo, P., "Modeling Cake Compressibility on Gas Filters," *High Temperature Gas Cleaning*, **2**, 83 (1999).
- Perry, R. H. and Green, D. W., "Perry's Chemical Engineers H/B," 6th ed., McGraw-Hill, 20 (1973).
- Schmidt, E., "Experimental Investigations into the Compression of Dust Cakes Deposited on Filter Media," *Filtration & Separation*, **September**, 789 (1995).
- Schmidt, E., "Theoretical Investigations into the Compression of Dust Cakes Deposited on Filter Media," *Filtration & Separation*, **May**, 365 (1997).
- Schulz, K. and Durst, M., "Advantages of an Integrated System for Hot Gas Filtration using Rigid Ceramic Elements," *Filtration & Separation*, **January/February**, 25 (1994).
- Silva, C. R. N., Negrini, V. S., Aguiar, J. R. and Coury, M. L., "Influence of Gas Velocity on Cake Formation and Detachment," *Powder Technology*, **101**, 165 (1999).